Teekaraman Yuvaraja, Mani Gopinath

New Gen Algorithm for Detecting Sag and Swell Voltages in Single Phase Inverter System for Micro grid

In this manuscript, a novel sag and peak detector by means of a delta square operation for a single-phase is suggested. The established sag detector is from a single phase digital phase-locked loop (DPLL) that is founded on a d-q transformation employing an all-pass filter (APF). The d-q transformation is typically employed in the three-phase coordinate system. The APF produces a virtual phase with a $90°$ phase delay, but the virtual phase can not reproduce an abrupt variation of the grid voltage, at the moment in which the voltage sag transpires. As a consequence, the peak value is severely garbled, and settles down gradually. A modified APF produces the virtual q-axis voltage factor from the difference between the current and the former value of the d-axis voltage component in the stationary reference frame. Nevertheless, the amended APF cannot sense the voltage sag and peak value when the sag transpires around the zero crossing points such as $0°$ and $180°$ since the difference voltage is not adequate to sense the voltage sag. The suggested algorithm is proficient to sense the sag voltage through all regions as well as the zero crossing voltage. Furthermore, the precise voltage drop can be obtained by computing the q-axis component, which is relational to the d-axis component. To authenticate the legitimacy of the suggested scheme, the orthodox and suggested approaches are contrasted by means of the simulations and investigational results.

Key words: All pass filter, Digital phase locked loop, Sag, Swells, Single phase inverter system

Novi gen algoritam za detekciju propada i poskoka napona na jednofaznom izmjenjivaču u mikromreži. U ovom radu je predložen novi detektor propada i poskoka napona korištenjem delta kvadratične operacije za jednu fazu. Predloženi detektor propada napona je u digitalnoj fazno-zatvorenoj petlji (DPLL) zasnovanoj na d-q transformaciji koja koristi svepropusni filtar (APF). D-q transformacija se tipično koristi u trofaznim koordinatnim sustavima. APF generira virtualnu fazu s $90°$ faznog kašnjenja, ali virtualna faza ne može reproducirati skokovitu promjenu napona mreže u trenutku u kojem se događa propad napona. Kao posljedica, detektirana vršna vrijednost se značajno izmijeni i smiruje se postepeno. Modificirani APF generira faktor napona virtualne q osi iz razlike između struje i prošle vrijednosti komponente napona na d osi u stacionarnom koordinatnom sustavu. Međutim, izmjenjeni APF ne može detektirati propad i poskok napona kada se propad događa u okolini točaka presijecanja nule, kao što je $0°$ i $180°$ s obzirom da diferencijski napon nije prikladan za detekciju propada napona. Predloženi algoritam je prilagođen detekciji propada napona u cijelom radnom području, uključujući i napon prelaska nule. Nadalje, precizni propad napona može se dobiti izračunom komponente napona na q osi, koja je u odnosu s obzirom na komponentu d osi. Za validaciju predloženih metoda provedena je njihova usporedba s konvencionalnim metodama u simulacijskom i eksperimentalnom okruženju.

Ključne riječi: svepropusni filtar, digitalna fazno-zatvorena petlja, propad, poskok, jednofazni izmjenjivač

1   INTRODUCTION

The pervasive computerization of crucial practices in business and production has led to a note worthy surge in the significance of strict voltage stability and control. Power quality in stabilities in the system, considerably influence sensitive loads and voltage sags are amongst the most recurrent power quality difficulties that upset power systems in the present day. Voltage sags are described as a decline in the root mean square (rms) voltage below 0.9pu of the nominal voltage at the power frequency for an extent extending from 0.5 cycles to 1 min [1]. It is imperative that the system senses the phase and amplitude of the grid voltage when a glitch be falls the grid. For this purpose, a sag voltage detector has been here to fore suggested [2]-[4].

Generally conventional peak detector methods have a time delay until recognition. The RMS technique has a time delay of 2-9 ms [5], the hybrid KF-RMS technique has a time delay of 0.5-4 ms [6], plus DVR has a 2ms time

delay [7]. Additional techniques report time delays stretching from 1-4 ms, with the maximum delay being produced at 0° or 180° for every technique. Of late, the fast peak detector has diminished, the typical detection delayed within 0.5ms for any phase, and three-five cycles sampling time is required [8]. Another established method is centered on the d-q transformation by means of an all-pass filter (APF). The APF produces a virtual phase with a 90° phase delay, but the virtual phase cannot reproduce sudden fluctuations in the grid voltage at the instant at which the voltage drop transpires. As a consequence, the peak value is drastically deformed and settles down gradually. Lately, a new sag sensing technique was realized employing the disparity among the present value and the former value of the grid voltage [8].

Nevertheless, the shortcoming of this technique is that, it takes time to sense the sag voltage, and it sometimes cannot sense the voltage sag around the zero crossing. To resolve these difficulties the novel sag detector is suggested in this manuscript. There are two difference voltages. Among them, one is the variance in the value between the current value and the former value, and the other variance voltage is the variance in the value between the current difference value and the subsequent difference value. The proposed sensing technique, entitled delta square operation, is realized by means of the difference voltages that exist between the two difference voltages. The projected technique reduces the delay in the typical detection time within one sampling time in any phase. This manuscript entails the succeeding three segments: the system configuration (APF) and digital phase-locked loop (DPLL), conventional detection method, and suggested detection method, simulations and investigational results.
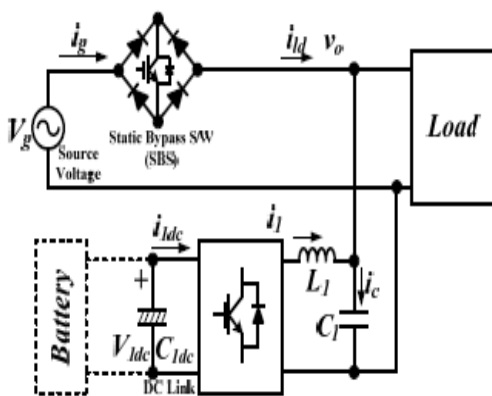

Fig. 1: Existing voltage compensation system

From Fig. 1, when the grid voltage is within the normal range, the static bypass switch is turned on, and it operates as an active power filter mode. When the grid voltage is out of the normal range, the static bypass switch is turned off,

and it operates as an uninterruptible power supply (UPS) mode. To achieve seamless mode transfer, the static bypass switch, which is consisted of an insulated-gate bipolar transistor (IGBT) and diode is used. However, if the grid voltage is not detected as soon as there is a voltage sag / swell, seamless mode transfer is not possible. Therefore, a new detection scheme that can detect the voltage drop is proposed.
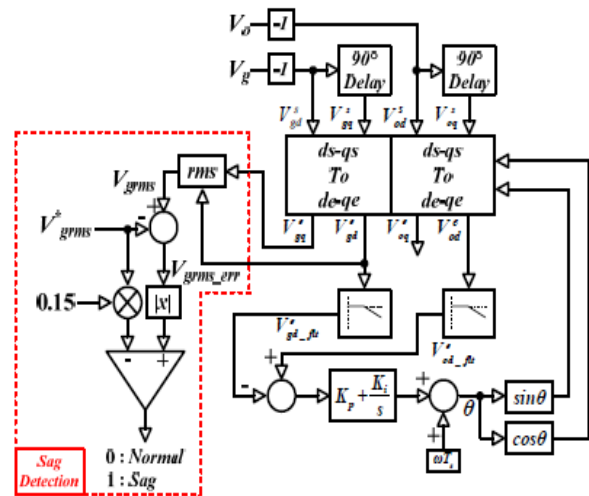
1.1 Conventional Sag Detector and DPLL

Fig. 2: Conventional sag detector and digital phase-locked-loop

Fig. 2 shows a conventional sag detector and the block diagram of a DPLL. V_{gd}^s is the d-axis component with the same magnitude and reverse phase as the grid voltage, and V_{gq}^s is the virtual q-axis component, which is generated using the APF from the grid voltage. The virtual phase V_{gq}^s can be obtained from the measured grid Voltage $V_{gd}^s = -V_g$ by using the APF in discrete time domain as follows:

$$V_{gd}^s(t) = -V_g(t) \tag{1}$$

$$V_{gq}^s(t) = -KV_{gqgd}^s s(t-1) + KV_{gd}^s(t) + V_{gd}^s(t-1) \tag{2}$$

$$K = \frac{T_{Samp.}}{T_{Samp.}} \frac{W-2}{W+2} \tag{3}$$

By using a synchronous rotating reference frame, the rms value of the grid voltage is obtained as follows.

$$V_{grms} = \sqrt{\frac{V_{gd}^e + V_{gq}^e}{2}} \tag{3}$$

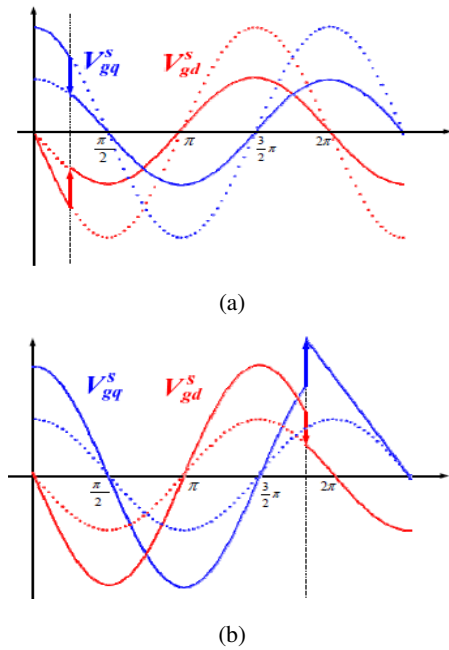$$V_{grms\,err} = V_{grms} - V_{grms}^* \tag{4}$$

(a)

(b)

Fig. 3: Features in All Pass Filter; a) Normal condition (0-90 degree, 180-270 degree); b) Isolated condition (90-180 degree, 270-360 degree)

If V_{grms_err} is beyond the 16% of the absolute source voltage (reference, $0.16 \times V_{grms}^*$), the source voltage sag is been detected. However, there is a delay in detecting the sag because of the non ideal condition of the all pass filter.

1.2   Conventional Modified APF

The modified APF is a technique used to check the grid voltage variation. The d-axis voltage component is generated from the current and previous values of the grid voltage, and the virtual q-axis component is generated using the same method. Fig. 4 shows a conventional sag detection scheme using the difference between the current and previous values of the voltage.

V_{gd}^s is the d-axis component with the same magnitude and reverse phase as the grid voltage, and V_{gq}^s is the virtual q-axis component, which is generated using the APF from the grid voltage. The virtual phase V_{gq}^s can be obtained from the measured grid voltage.

$$\Delta V_{gd}^s = V_{gd}^s(t) - V_{gd}^s(t-1) = -A\sqrt{2}\,\cos(wt - \alpha) \tag{5}$$
$$\Delta V_{gq}^s = V_{gq}^s(t) - V_{gq}^s(t-1) = -A\sqrt{2}\sin(wt - \alpha) \tag{6}$$

Where $\alpha = 2\pi f\, T_{samp} \cdot 0.5$ and $A = V_g \cdot Sin\alpha \cdot 2 V_{gd}^s(t-1)$, $V_{gq}^s(t-1)$ are the values for one step ahead voltage. ΔV_{gd}^s is equal to $-A\sqrt{2}\cos wt$, and the magnitude is much smaller than the real grid voltage. The peak
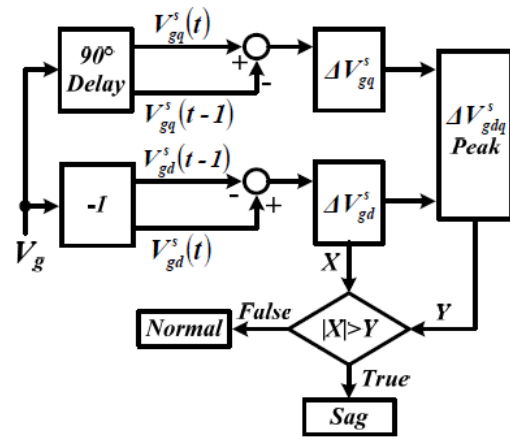

Fig. 4: Conventional sag detection scheme using the difference between current and previous values of the voltage

value of the grid voltage, $\Delta V_{gdq\,peak}^s$ is calculated under normal condition, and is

$$\Delta V_{gdq\,peak}^s = \sqrt{(\Delta V_{gd}^s)' + (\Delta V_{gq}^s)'} = A\sqrt{2} \tag{7}$$

ΔV_{gd}^s is then compared with $\Delta V_{gdq\,peak}^s$, and is $\left| \Delta V_{gd}^s \right| > \Delta V_{gdq\,peak}^s$, then it means that a sag had occurred.

However, as shown in Fig. 5 and Table I, when the sag occurred at around zero voltage, it cannot be detected because the variation in the voltage is small owing to the characteristic of the sinusoidal waveform.

Table 1: System parameters

Voltage Sag	T_{samp} = 100 μs	T_{samp} = 100 μs
10%	$\pm$ 22.2° (1.02ms)	$\pm$ 42.5° (2.22ms)
20%	$\pm$ 10.5° (500ms)	$\pm$ 2.2° (1.03ms)
30%	$\pm$ 7.1° (330ms)	$\pm$ 14.2° (670ms)
40%	$\pm$ 5.5° (249ms)	$\pm$ 10.3° (502ms)
50%	$\pm$ 4.6° (200ms)	$\pm$ 8.1° (404ms)

The parameters of y-axis in Fig.5 are the mean amplitude of sine function.

For example, at 10% of the sag voltage when the sampling time is 100 μs, sags within $\pm$22.1° were not detected, and at 50% of the sag voltage when the sampling time is 100 μs, sags within $\pm$4.3° were not detected. If the sampling time is increased to 200 μs, the length of time needed before detecting the sag voltage is much longer.

1.3   Proposed Sag/Peak Detection Method

Fig. 6 shows the block diagram for the proposed sag detection, and the virtual new q-axis voltage, $V_{gd\,n}^s$ can be
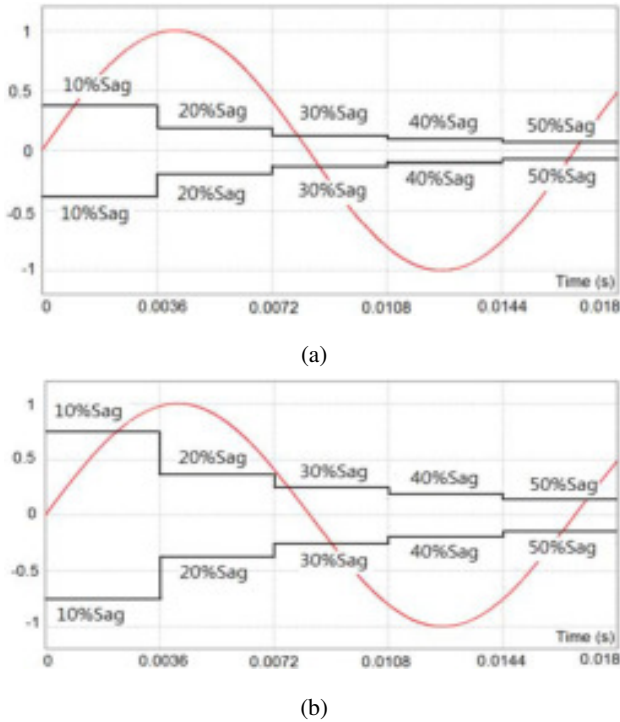
(a)

(b)

Fig. 5: Sag detection range of the source voltage depending on the voltage sag; (a) when the sampling time is 100 μs, (b) when the sampling time is 200 μs

Fig. 6: Proposed detection of Sag Scheme

acquired using the proposed method. The 1st components of the difference voltages are generated through ΔV_{gd}^s and ΔV_{gq}^s, which are based on the value of the present / one step ahead for V_{gd}^s and V_{gq}^s respectively. In the same manners as Equations. (5) And (6), the 2nd components of the difference voltage are acquired as follows.

$$\Delta \left(\Delta V_{gd}^s (t) \right) = \Delta V_{gd}^s (t) - \Delta_{gd}^s (t-1) = B\sqrt{2}\sin(wt) \quad (8)$$

$$\Delta(\Delta V_{gq}^s(t)) = \Delta V_{gq}^s (t) - \Delta V_{gq}^s(t-1) = -B\sqrt{2}\cos wt \quad (9)$$

Where $\alpha = 2\pi f$, $T_{samp} \cdot 0.5$, $B = A \cdot 2\alpha$.

The peak value of the grid voltage $\Delta(\Delta V_{gdq}^s)_{peak}$ is calculated under normal conditions. The peak value can be found, as follows:

$$\Delta(\Delta V_{gdq}^s)_{peak} = B\sqrt{2} \quad (10)$$

$\Delta(\Delta V_{gdq}^s)_{peak}$ is the peak value of the grid voltage, and is updated every hour under normal conditions. By comparing $\Delta(\Delta V_{gdq}^s)_{peak}$ with ΔV_{gd}^s, if ΔV_{gd}^s is existed with $\pm \Delta(\Delta V_{gdq}^s)_{peak}$, the grid voltage is normal, but if ΔV_{gd}^s becomes greater than $\pm \Delta(\Delta V_{gdq}^s)_{peak}$ then there is a failure. After recognizing the failure, the system calculates
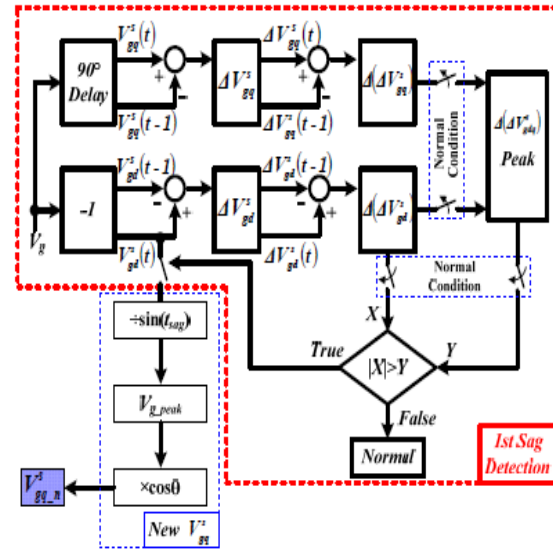
the peak value of grid voltage, as shown in equation (11). It means the sag occurs the peak voltage of the grid can be calculated by using the grid voltage and phase. The virtual phase $V_{gq\_n}^s$ can be obtained by using the peak voltage of grid voltage and virtual phase.

$$V_{g\_peak} = \left| \frac{V_{gd}^s (t_{sag})}{\sin(t_{sag})} \right| = \left| \frac{-V_m \sin(t_{sag})}{\sin(t_{sag})} \right| \quad (11)$$

The virtual phase $V_{gq\_n}^s$ has been obtained from the measured grid voltage by using the eq. (12).

$$V_{gq}^s (t_{sag}) = V_{g\_peak} \times \cos(\theta_{sag}) = V_{gq\_n}^s \quad (12)$$

As shown in Fig. 7, the new-peak value is created through the output of the rotating co-ordinate system using this $V_{gq\_n}^s$. The system detects the sag immediately because of this peak value..

The all pass filter generates a proper virtual phase when the sag occurs between $0°$ to $90°$ and between $180°$ to $270°$. But when the sag occurs between $270°$ to $360°$, the all pass filter generates the wrong virtual phase.

Assume that a fixed percentage, x, of the voltage sag occurred at time $(t+1)$. Then the following equations apply:

$$V_{gd}^s (t-1) = -\sqrt{2}V \sin(\omega t - 2\alpha)$$

$$V_{gd}^s (t) = -\sqrt{2}V \sin \omega t \quad (13)$$

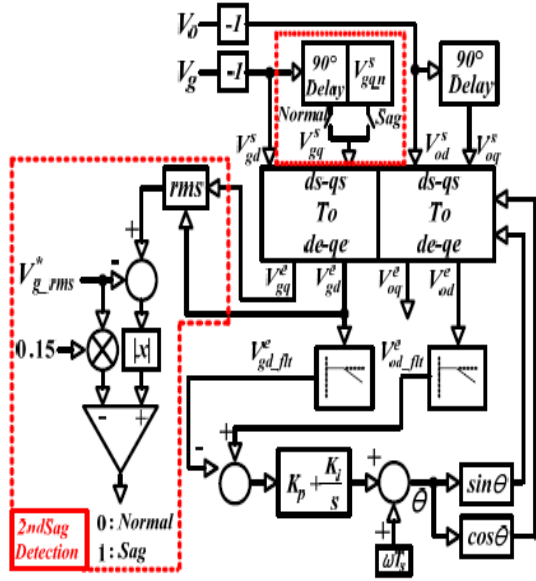$$V_{gd}^s (t+1) = -\sqrt{2}V (1-x)\sin(\omega t + 2\alpha)$$

Fig. 7: Proposed sag/peak detection using the new $V_{gq\_n}^s$

Based on the value of the present/one step ahead for V_{gd}^s and V_{gq}^s, the first component of the change was generated through ΔV_{gd}^s and ΔV_{gq}^s, respectively.

$$\Delta V_{gd}^s(t) = V_{gd}^s(t) - V_{gd}^s(t+1) \cong -A\sqrt{2}\cos\omega t \quad (14)$$

$$\Delta V_{gd}^s(t+1) = V_{gd}^s(t+1) - V_{gd}^s(t)$$

$$\cong -\sqrt{2}V\left(-x\sin\omega t + 2\alpha\{1-x\}\cos\omega t\right) \quad (15)$$

The difference voltage of the second component was generated by $\Delta V_{gd}^s(t+1)$ and $\Delta v_{gd}^s(t)$.

$$\Delta\left[\Delta V_{gd}^s(t+1)\right] = \Delta V_{gd}^s(t+1) - \Delta V_{gd}^s(t)$$

$$= \sqrt{2}V\,x\,(\sin\omega t + 2\alpha\cos\omega t) \quad (16)$$

The minimum voltage drop which can be detected at t=0 and it is calculated as follows.

$$\Delta\left[\Delta V_{gd}^s(1)\right] = \sqrt{2}V\,x\,(\sin 0 + 2\alpha\cos 0)$$
$$= \sqrt{2}V\,x\,2\alpha = B\sqrt{2} \quad (17)$$

$$X = \frac{B\sqrt{2}}{\sqrt{2}\,V\,2\alpha} \quad (18)$$

The minimum detection level of the sag voltage can be manipulated using B.

## 1.4 Solution for the noise and harmonics on the grid side

However, the proposed method has a disadvantage with respect to the noise and harmonics of the grid side, because when detecting the grid voltage, the difference in the difference voltage is used. Therefore, when detecting the grid voltage -40 dB/dec low-passes Butterworth filter used in the controller implementation are realized with a cut-off frequency of 5.1 kHz. The phase delay of the filter is about 60 μs at the fundamental frequency.

2 SIMULATION RESULTS

The simulation of the proposed algorithm has been performed in power simulation. The sag voltage dropped to 50% of its nominal value.

Fig. 9 shows the characteristics of the APF when the sag / swell occur at a specific phase. As shown in Fig. 9(a) and 9(b), the APF generates a proper virtual phase when the sag / swell occurs between 0° and 90°, and between 180° and 270°, respectively. In this case, the polarities of V_{gd}^s and V_{gq}^s are the opposite of each other. However, Fig. 9(c) and 9(d) show that the APF generates opposite virtual phases when the sag / swell occurs between 90° and 180°, and between 270° and 360°, respectively. In this case, the polarities of V_{gd}^s and V_{gq}^s are the same.

Fig. 10 shows the grid voltage obtained for the conventional method using the d-q transformation at 60° when sagged by 50%. Fig. 10(a) shows V_{gd}^s from the grid voltage and a 90° phase-lagged virtual waveform V_{gq}^s generated by the APF. When V_{gd}^s sags at 60°, V_{gq}^s reflects the proper sag voltage value, as shown in Fig. 10(a). In other words, when the grid voltage decreased by 50% at 60°, the virtual phase V_{gq}^s also decreased.
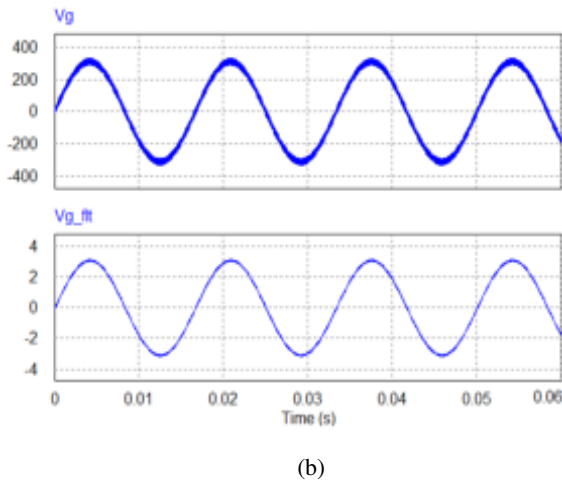

(a)

(b)
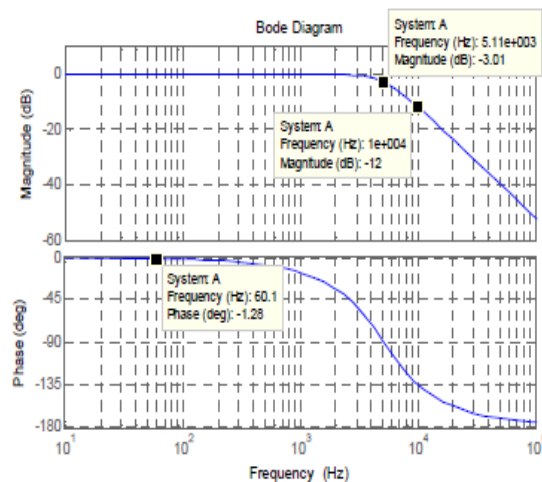
Fig. 8: Characteristics of the low-pass filter; (a) frequency domain, (b) time domain
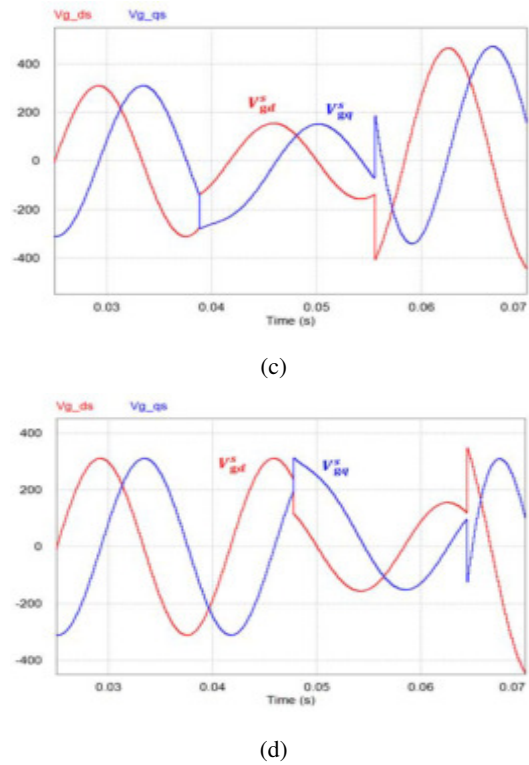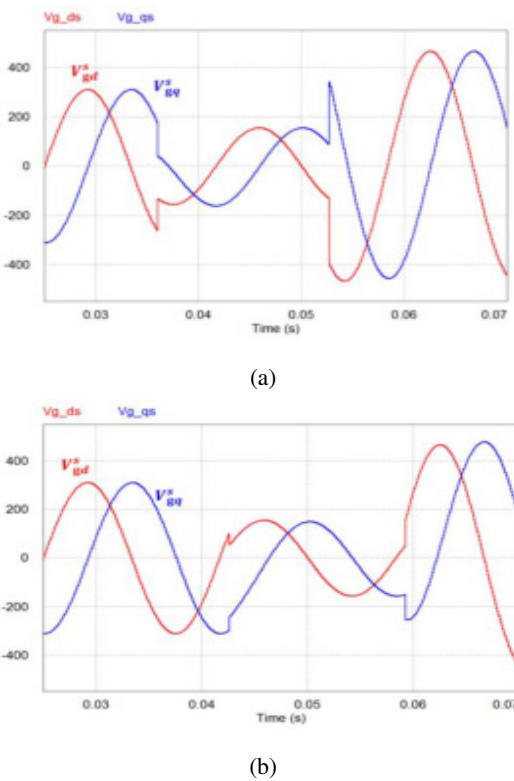

(c)

(d)

Fig. 9: 50% sagged/swelled grid voltage for the conventional all-pass filter; (a) sagged/swelled grid voltage at 60°, (b) sagged/swelled grid voltage at 200°, (c) sagged/swelled grid voltage at 120°, (d) sagged/swelled grid voltage at 310°

Fig. 10(b) shows the sag voltage detection level. The sag is detected when the source voltage drops to 15% of the nominal rms value. Fig. 10(c) shows the rms value of the grid voltage in Eqs. (3) and (4). Fig. 10(d) shows the detected blackout signal. Because of the proper virtual waveform of V_{gq}^s, the sag voltage was detected properly.

Fig. 11 shows the grid voltage for the conventional

(a)

(b)

method obtained using the d-q transformation at 310° when sagged by 50%. When V_{gd}^s sags at 310°, V_{gq}^s reflects the wrong sag voltage value, as shown in Fig. 11(a). Namely, when the grid voltage decreased by 50% at 310°, the virtual phase V_{gq}^s increased. Therefore, it takes time to calculate the rms value of the grid voltage. The blackout signal (BS) is represented by a zero (0) when the system is normal conditions, and if the system is abnormal conditions, the BS is represented by one (1).

Fig. 12 shows the sag detection characteristic at 60° when the difference voltage between the current and previous values is used. The values of $V_{gq\_n}^s$, ΔV_{gd}^s, $\Delta\left(\Delta V_{gd}^s\right)$, $\Delta V_{gdg\_peak}^s$, and $\Delta\left(\Delta V_{gdg}^s\right)_{peak}$ come from Equations. (12), (5), (7), (8), and (10), respectively.

Fig.12 (a) shows the voltage sag detection characteristic when the difference voltage between the current and previous values of the d-axis voltage component is used in the stationary reference frame. The d-axis voltage component (V_{gd}^s) is the same as the grid voltage (-V_g). The value of ΔV_{gd}^s is compared with $\Delta V_{gdqpeak}^s$.
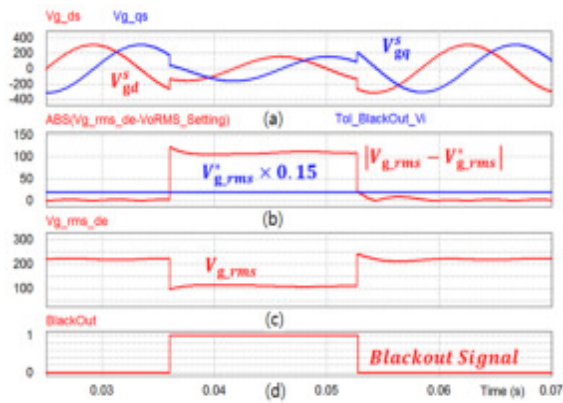
Fig. 10: 50% sagged/returned grid voltage for the conventional method at 60°; (a) stationary reference frame, (b) sag detection level, (c) detected rms voltage, (d) b0lackout signal
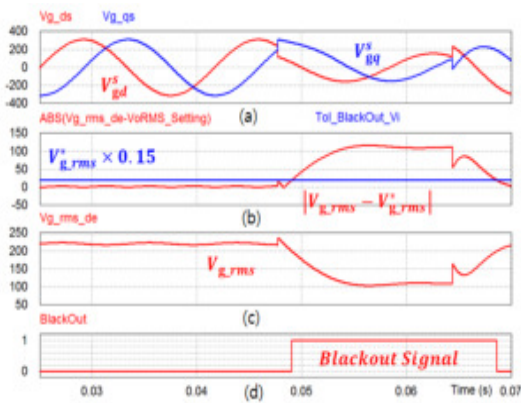

Fig. 11: 50% sagged/returned grid voltage for the conventional method at 310°; (a) stationary reference frame, (b) sag detection level, (c) detected rms voltage, (d) Blackout signal

If $\left| \Delta V_{gd}^s \right| \triangleright \Delta V_{gdqpeak}^s$, it indicates that the sag occurs as shown in Fig. 12(b). Fig.12(c) shows the proposed method. The result is almost the same as that obtained with the conventional method. Fig. 13 shows the voltage sag detection characteristic at 0°. Fig. 13(b) shows that the voltage sag is not detected, because the difference voltage between the current and previous values is not above the peak voltage level. This is because the source voltage is about zero, while the difference voltage is also too small. However, as shown in Fig. 13(c), the proposed method detects the voltage sag. Because of the voltage detection, the virtual q-axis voltage component. The proposed sag / peak detection methods were shown in Fig. 14 to Fig. 17. The value of Vg_peak is the peak of the grid voltage ob-
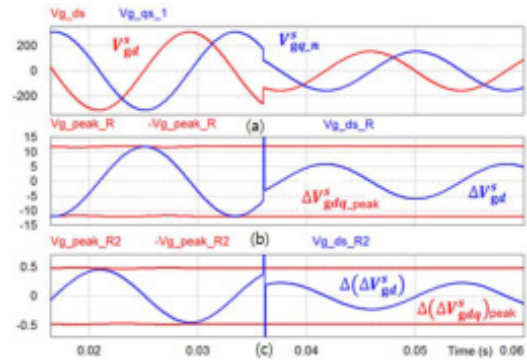

Fig. 12: Voltage sag detection characteristic around 60° when the difference voltage between the current and previous values is used. (a) (b) (c)
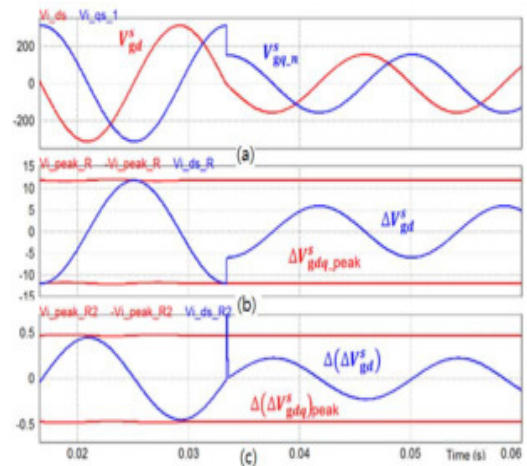

Fig. 13: Voltage sag detection characteristic at 0°, when the difference voltage between, the current and previous values is used
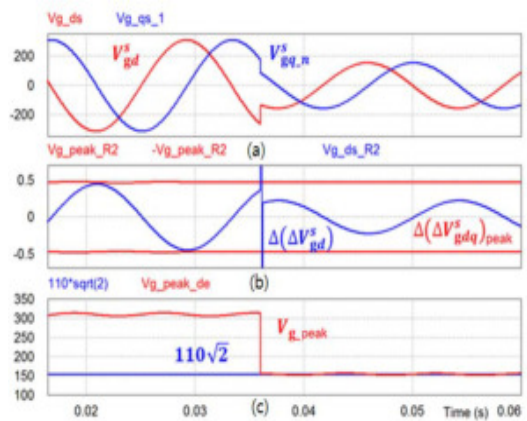

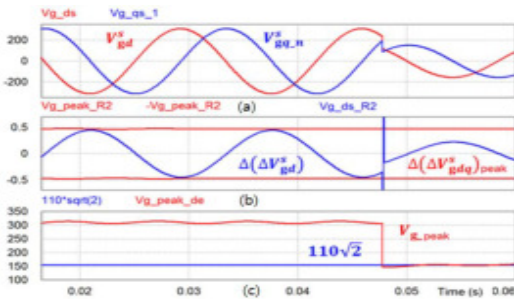Fig. 14: 50% sagged grid voltage at 60°

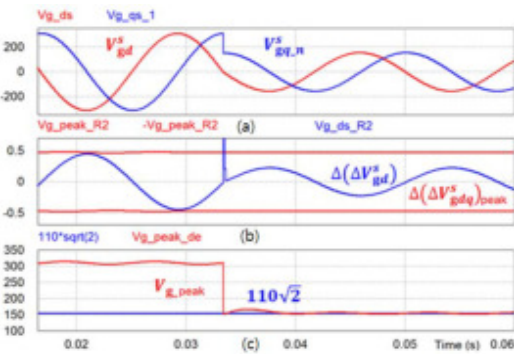Fig. 15: 50% sagged grid voltage at 310°
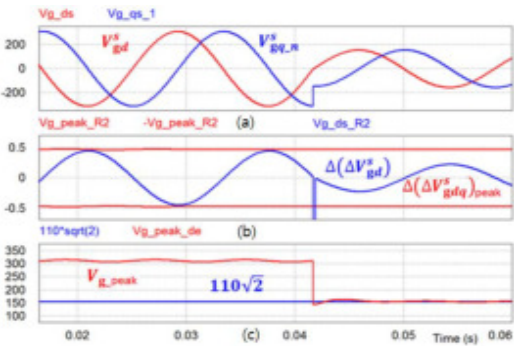

Fig. 16: 50% sagged grid voltage at 0°

Fig. 17: 50% sagged grid voltage at 180°

tained using the synchronous d-q transformation. When the sag occurs at 60°, 310, 0°, and 180°, the sag was detected. Because of the sag detection, the peak grid voltage was acquired immediately.

3   EXPERIMENTAL RESULTS

In order to verify the proposed strategy the algorithm was implemented using a digital signal processor (TMS320C33). A single 32 bit floating point DSP with a single cycle execution time of 13.3 ns was used, and the switching period of the PWM is 100 micro sec. The system parameters are shown in table 1. The nominal input

voltage was 209v, voltage sags were simulated with a tap changing transformer and switching device, so that various voltage levels could be generated. In this, the source voltage was decreased from 209V to 102V during sag event.
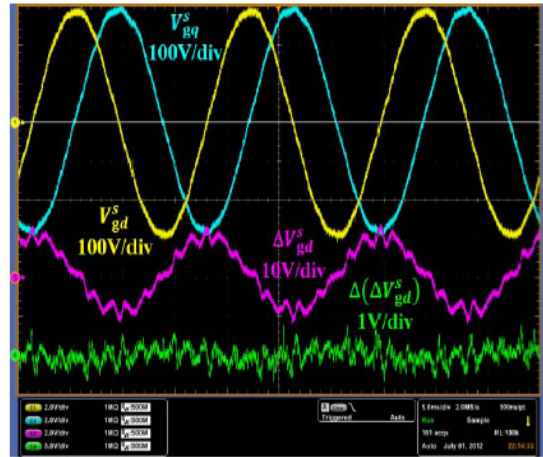

Fig. 18: Experimental Results on Grid Voltage; Ch1: V_{gd}^s grid voltage (100v/div), Ch2: V_{gq}^s virtual voltage source, Ch3: ΔV_{gd}^s conventional difference voltage, Ch4: $\Delta\left(\Delta V_{gd}^s\right)$ proposed difference voltage

Fig.18. shows the derived components obtained from the grid voltage. The waveform of the d-axis voltage component V_{gd}^s and q-axis voltage component V_{gq}^s are little distorted, and the difference voltages $\left(\Delta V_{gd}^s,\ \Delta\left(\Delta V_{gd}^s\right)\right)$ are significantly distorted.
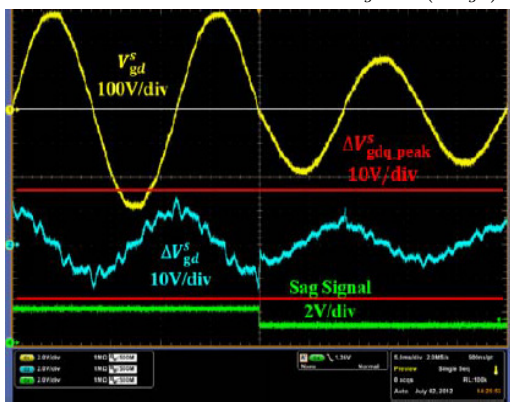

Fig. 19: Harmonic Analyzer

Fig.19. shows the harmonic analysis results of grid voltage. In this the grid voltage includes the third, fifth, seventh harmonic components. Finally it concludes the difference voltages are distorted.
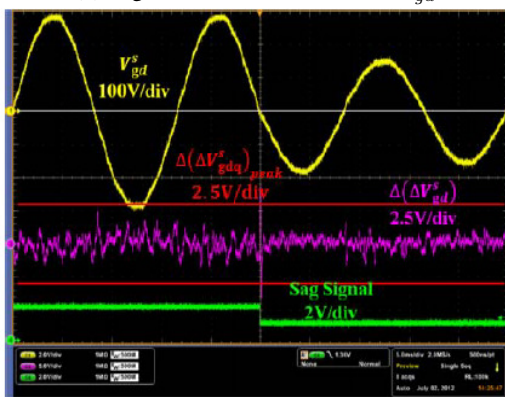
Fig.20 shows the sag detection waveform that was used
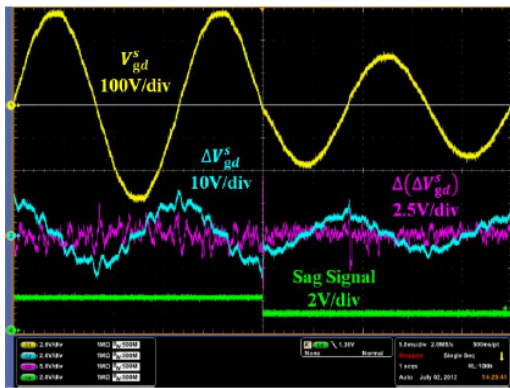
(a) Sag detection waveform for ΔV_{gd}^s, $\Delta\left(\Delta V_{gd}^s\right)$


(b) Sag detection waveform for ΔV_{gd}^s,

(c) Sag detection waveform for $\Delta\left(\Delta V_{gd}^s\right)$

Fig. 20: Comparison of Sag detection waveform for V_{gd}^s, $\Delta\left(\Delta V_{gd}^s\right)$ for 2.5/division

to compare V_{gd}^s, with $\Delta\left(\Delta V_{gd}^s\right)$. The sag occurred at 0 degree in Fig. 20 (b). The occurrence of sag can be detected is ΔV_{gd}^s and $\Delta\left(\Delta V_{gd}^s\right)$ matches each peak value. However in the cases of fig 20(b) the variation in ΔV_{gd}^s was too small to detect the sag. On the other hand in the case

of fig.20(c), the sag detection becomes possible because $\Delta\left(\Delta V_{gd}^s\right)$ matched the peak value of $\Delta\left(\Delta V_{gd}^s\right)$. The sag signal of Ch 4 was output when the system recognized the sag. During the normal conditions, the value maintains by 2V and if there is a problem with the grid voltage, the sag-signal changes by 1V.
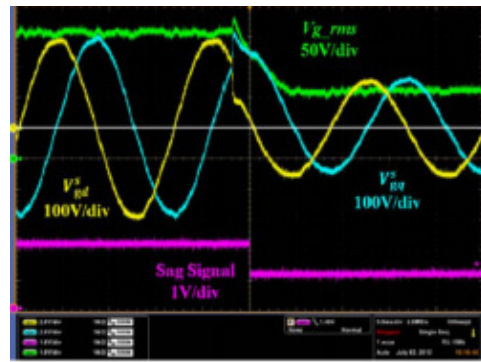
(a) The occurrence of Sag at $310°$ using the conventional method
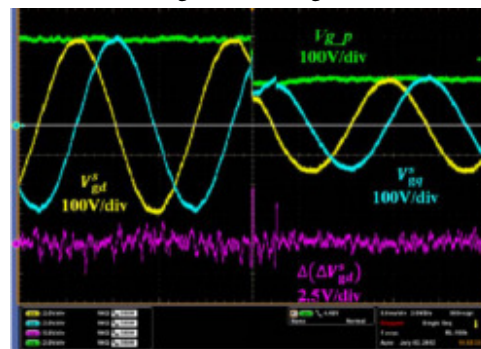
(b) The occurrence of Sag at $310°$ using the proposed method
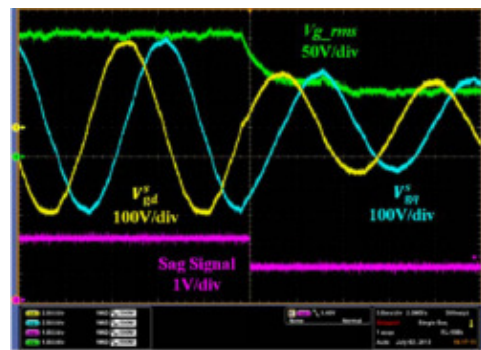
(c) The occurrence of Sag at $180°$ using the conventional method

Fig. 21 shows a comparison of the conventional and proposed methods. In this the grid voltage decreased from 209V to 102V during the event. Fig. 21(a) shows the conventional method. When V_{gd}^s sags at $310°$, V_{gq}^s reflects the wrong sag voltage value, which is shown. So grid voltage decreased by 50% at $310°$, the virtual phase V_{gq}^s increased. The time taken to calculate the rms value of grid voltage.
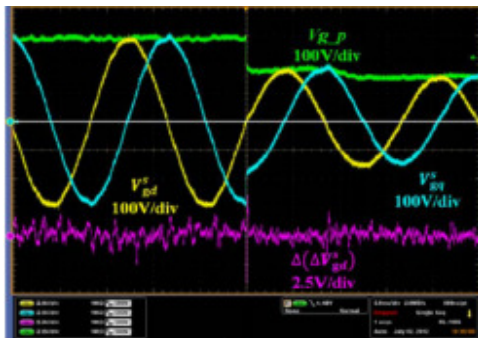
(d) The occurrence of Sag at $180°$ using the proposed method

Fig. 21: (a), (b), (c), (d) comparison of waveform for sag detections

Fig. 21 (b) shows the proposed method value, which the grid voltage decreased by 50% at $310°$, the sag was immediately detected, and the virtual phase V_{gq}^s decreased and the rms value of the grid voltage is also calculated immediately. Fig. 21 (c)(d) is as same as.

4 CONCLUSION

Through this paper, the new sag and peak detector for a single phase was proposed. The conventional sag detector is from a single-phase DPLL that is based on a d-q transformation using an APF. The APF generates a virtual phase with a $90°$ phase delay, but the virtual phase cannot reflect sudden changes in the grid voltage at the instant of voltage sags between $0°$ and $90°$, and between $180°$ and $270°$. As a result, the peak value is significantly distorted, and settles down slowly. Moreover, the settling time of the peak value is too long.

To reduce these delays, the difference voltage between the current and previous values of the voltage component was used in the stationary reference frame, but the system cannot recognize the sag around the zero-crossing point. Therefore, the proposed method used the difference voltage of the 2nd component between the difference of the current value, and difference of one step ahead. The proposed algorithm is possible to detect the sag voltage through all regions including the zero crossing voltage. Moreover, the exact voltage drop can be acquired by calculating the q-axis component, which is proportional to the d-axis component. The control algorithm and mathematical models were proposed, and simulation and experiment results were presented to verify the performance of the proposed control strategy. The proposed algorithm will be applied to a real inverter system in order to verify its application in the field.

REFERENCES

[1] R. Naidoo, P. Pilay, "A New Method of Voltage Sag and Swell Detection," *IEEE Trans. on Power Delivery*, Vol. 22, No. 2, pp. 1056-1063, Apr. 2007.

[2] N. Woodley, L. Morgan, A. Sundaram, "Experience with an Inverter-based dynamic voltage restorer," *IEEE Trans. on Power Delivery*, Vol. 14, No. 3, pp.1181-1186, July. 1999.

[3] W. Lee, D. Lee, T. Lee, "New Control Scheme for a Unified Power Quality Compensator-Q with Minimum Active Power Injection," *IEEE Trans. on Power Delivery*, Vol. 25, No. 2, pp. 1068-1076, Apr. 2010.

[4] W. Lee, W. Lee, T. Lee, "Integrated inverter system for compensation of Power Quality events," *Power Electronics Specialists Conference*, pp. 3754-3759, June. 2008.

[5] N. Tuaboylu, E. Collins, P. Chaney, "Voltage Disturbance Evaluation Using the Missing Voltage Technique", Harmonics and Quality of Power, Vol. 1, pp. 577-582, 1998.

[6] M. Gonzalez, V.Cardenas, R. Alvarez, "A Fast Detection Algorithm for Sags, Swells, and Interruptions Based on Digital RMS Calculation and Kalman Filtering," *in Proc. Int. Power Electronics Congress*, pp. 1-6, Oct. 2006

[7] Z. Yao, L Xiao, "Seamless transfer of single-phase grid-interactive inverters between grid-connected and stand-alone modes," *IEEE Trans. on Power Electronics*, Vol. 25, No. 6, pp. 1597-1603, 2010.

[8] Y. Silla, Y. Kum, "An Improvement in Synchronously Rotating Reference Frame-Based Voltage Sag Detection under Distorted Grid Voltages," *Journal of Power Electronics*, Vol. 8, No. 6, pp. 1283-1295, 2013.

[9] S. Lee, K. Sung, T. Lee, W. Lee "UPS/APF power conversion equipment with a seamless mode transfer," *Energy Conversion Congress and Exposition (ECCE),* pp. 2769 – 2776, May 2011.

Teekaraman Yuvaraja has obtained his B.E degree from Anna University, Chennai in the year 2009. He obtained his M.E degree from Anna university, chennai in the year 2012. Currently he is pursuing as Research Scholar in the Department of Electrical and Electronics Engineering in Meenakshi Academy of Higher Education and Research, Chennai, India. His research interests include electromagnetic transients in power systems, power electronics and power system dynamics and control.

Mani Gopinath has obtained his B.E degree from Bharathiar University, Coimbatore in the year 2002. He obtained his M-Tech degree from Vellore Institute of Technology; Vellore in the year 2004.He obtained is Doctorate from Bharath University, Chennai. He is working as a Professor/EEE, at Dr.N.G.P Institute of Technology, Coimbatore, India. His Area of interest is Power Electronics. He is professional member of IEEE, ISTE, IETE, IAENG, and IACSIT. He has received best performer award in the year 2010.

AUTHORS' ADDRESSES
Teekaraman Yuvaraja, M.Sc.E.E.
Department of Electrical and Electronics Engineering,
Meenakshi Academy of Higher Education and Research,
600 078 Chennai, India
email: yuvarajastr@gmail.com

Prof. Mani Gopinath, Ph.D.
Department of Electrical and Electronics Engineering,
Dr.N.G.P Institute of Technology,
641 048 Coimbatore, India
email: gopinath@drngpit.ac.in